

Jet impingement quenching phenomena for hot surfaces well above the limiting temperature for solid–liquid contact

Md. Ashraful Islam^a, Masanori Monde^{a,*}, Peter Lloyd Woodfield^b, Yuichi Mitsutake^a

^a Department of Mechanical Engineering, Saga University, 1 Honjo, Saga-840 8502, Japan

^b Institute of Ocean Energy, Saga University, 1 Houjo, Saga 840 8502, Japan

Received 19 June 2006

Available online 8 January 2008

Abstract

Experiments were conducted to understand the phenomena that happen just after a subcooled free-surface circular water jet impinges on a high temperature surface. A 2 mm-water-jet of 5–80 K subcooling and 3–15 m/s velocity was impinged on the flat surface of a cylindrical steel/brass block that was preheated to 500–600 °C. The transient temperature data were recorded and used to predict the surface temperature by an inverse heat conduction technique. A high-speed video camera was also employed to capture the flow condition. It is found that for a certain period of time the surface temperature remains well above the thermodynamic limiting temperature that allows stable solid–liquid contact. What happens during this period and what makes the surface temperature drop to the limiting temperature are important questions whose possible answers are given in this article. The cooling curves at the center of the impinging surface for different experimental conditions are also explained in relation with the limiting temperature and three characteristic regions having different types of flow patterns are identified.

© 2007 Published by Elsevier Ltd.

Keywords: Boiling; Jet impingement quenching; Homogeneous nucleation; Solid–liquid contact

1. Introduction

Jet impingement quenching has a high cooling potential (more than 10 MW/m²) and is a very effective means of cooling. It is very important in LOCA analysis, steel manufacturing, metallurgy, microelectronic device making and thermal management processes. It may be useful in elucidating poorly understood phenomena such as Leidenfrost and homogeneous nucleation. A comprehensive review of jet impingement boiling was made by Wolf et al. [1]. They observed that in contrast to research on nucleate boiling and critical heat flux, there is a scarcity of concrete studies relating to jet impingement for the film boiling and transi-

tion regimes. Monde et al. [2] also surveyed a great many experimental studies on jet impingement quenching and made a comprehensive summary.

Heating a surface, that is submerged in a liquid pool, above the saturation temperature may give rise to heterogeneous nucleation or homogeneous nucleation of bubbles at the interface between the liquid and the solid. Even though the homogeneous nucleation of vapor has been studied extensively and has a rather long history of investigation, there is much not yet understood. Conventional homogeneous nucleation theory suggests that the homogeneous nucleation is likely to occur at the solid surface where the liquid is quickly and highly superheated. Skripov [3] and Asai [4] mentioned about spontaneous nucleation due to thermal motions of liquid molecules (homogeneous nucleation) under extremely high heat flux pulse heating cases. Andrews and O'Horo [5] observed bubble formation by homogeneous nucleation on or near the heater surface

* Corresponding author. Tel.: +81 952 28 8608; fax: +81 952 28 8587.

E-mail addresses: ashraful@me.saga-u.ac.jp (M.A. Islam), monde@me.saga-u.ac.jp (M. Monde), peter@me.saga-u.ac.jp (P.L. Woodfield), mitsutake@me.saga-u.ac.jp (Y. Mitsutake).

Nomenclature

c	specific heat (J/kg K)	T_{shn}	spontaneous homogeneous nucleation temperature (°C)
d	jet diameter (mm)	T_{tls}	thermodynamic limit of superheat of liquid (°C)
q	heat flux (MW/m ²)	T_{w}^*	surface temperature at t^* (°C)
r	radial position (mm)	u	jet velocity (m/s)
t	time (s)	ΔT_{sub}	liquid subcooling = $(T_{\text{sat}} - T_1)$ (K)
t^*	resident time (s)	ΔT_{sat}	surface or wall superheat = $(T_{\text{w}} - T_{\text{sat}})$ (K)
T	temperature (°C)	λ	thermal conductivity (W/m K)
T^*	solid–liquid interface temperature (°C)	ρ	density (kg/m ³)
T_{b0}	block initial temperature (°C)	<i>Subscripts</i>	
T_{c}	critical temperature (°C)	g	gas or vapor
T_{max}	maximum solid temperature that allows stable solid–liquid contact (°C)	l	liquid
T_{Leid}	Leidenfrost temperature (°C)	s	solid
T_{sat}	saturation temperature of liquid (°C)	w	wall or surface
T_{spin}	temperature at the liquid spinodal (°C)		

during the heating transient. They reported the occurrence of homogeneous nucleation away from the surface which would seem to contradict the expectation that homogeneous nucleation, if it occurs, will take place first at the surface itself where the liquid is superheated the most. Carey et al. [6] argued that for this observation [5] to be correct, there would have to be a mechanism that suppresses homogeneous nucleation very near the wall, or makes it more likely some distance away from it. One possibility they pointed out is that force interactions between molecules of the liquid and molecules in the solid surface are affecting the state of the fluid in a way that modifies the intrinsic stability limit. Gerweck and Yadigaroglu [7] developed an analytical model of the effects of attractive forces on the equation of state of the fluid. They used a thermodynamic analysis to assemble an equation of state by combining a repulsive force interaction model for a hard sphere fluid with attractive force models for interactions between the fluid molecules and solid surface molecules. Their analysis is cast in terms of an inverse characteristic length and concluded that the length scale is of the order of a molecular diameter, but no specific values were provided. Carey and Wemhoff [6] started from the interesting insight of Gerweck and Yadigaroglu [7] and developed a thermodynamic model stating that near-wall effects on nucleation and boiling are confined to the region within a few nanometers of the surface where pressure and spinodal temperature (T_{spin}) are extremely high. This implies that during transient heating, the homogeneous nucleation seems to occur first at a location slightly away from the solid surface free from near-wall effects. It is to be noted that at the wall-unaffected region, the bulk liquid can give rise to homogeneous nucleation of bubbles near the spinodal limit (T_{spin} which may otherwise be called T_{tls} noting that this temperature corresponds to the thermodynamic limiting superheat).

Ohtake and Koizumi [8] studied the mechanism of vapor-film collapse at the wall temperature above the spin-

odal limit (T_{tls}). They pointed out that local solid surface temperature at the position of solid–liquid contact could never exceed the T_{tls} or the spontaneous homogeneous nucleation temperature (T_{shn}) even if the vapor-film collapse occurred at a high wall-superheat. They also reported the effects of a local-cold spot on both the minimum-heat-flux (MHF) temperature and the way in which the vapor film would collapse. From the abovementioned survey, it seems that T_{tls} , T_{shn} , T_{Leid} and MHF-point temperature in relation with phase-change may demonstrate a physical phenomenon (homogeneous nucleation or Leidenfrost behavior) yet to be addressed clearly.

Jet impingement cooling of a hot surface may also give rise the heterogeneous and homogeneous nucleation of bubbles, which is yet to be explored. A number of interesting phenomena have been reported for jet impingement quenching. Piggott et al. [9] reported a delay to the movement of the wetting front during quenching heated rods from an initial temperature of 700 °C with a subcooled water jet. The quench began with quiet film boiling and then a white patch around 5 mm in diameter appeared beneath the jet. The liquid film then broke into tiny droplets in a spray pattern, which was followed by an oscillating liquid sheet that lifted from the surface of the rod. Finally, the wetting front moved forward over the heated surface. Some more recent works include Hammad et al. [10,11], Woodfield et al. [12], Mozumder et al. [13,14]. These recent studies have been performed by quenching a cylindrical block of initial temperature ranging from 250 to 400 °C. These studies emphasized on flow visualization, surface temperature, surface heat flux, cooling curves, boiling curves, resident time (wetting delay) and boiling sound.

Film boiling region is common at the early stages of jet impingement quenching of high temperature surfaces. Ishigai et al. [15] observed no solid–liquid contact in the film boiling region. The beginning of the contact is often understood to coincide with the minimum heat flux point. Many

studies have been done by assuming a continuous vapor film existing between the liquid and hot surface throughout the film boiling region. Some studies have shown that brief random contacts between the liquid and the surface occur in some portions of this region [16]. Chang and Witte [16] argued that the vapor film might appear to be quite continuous to the naked eye, but small contacts become longer and more numerous as the wall superheat approaches that at minimum heat flux. The liquid–solid contacts contribute to the average heat transfer rate during this stage of film boiling, eventually leading to the so-called minimum heat flux. They reported random solid–liquid contacts during flow film boiling measured with a surface micro-thermocouple probe. Hatta et al. [17] conducted jet quenching experiments of stainless steel plate initially heated to 900 °C and concluded that direct solid–liquid contact occurred without any noticeable period of film boiling in spite of the high temperature. Cokmez-Tuzla et al. [18] utilized a special rapid-response probe to detect and record potential liquid contacts during post-CHF flow boiling.

From the above mentioned studies it is clear that jet impingement quenching phenomena in the high temperature context are not well understood. Moreover, the nature of solid–liquid contact during quenching very hot surfaces is not known completely. In the present study these issues are addressed during jet impingement quenching of high temperature block having initial temperature from 450 to 600 °C. Steel and brass blocks are quenched by a 2 mm circular free surface water jet of velocity 3–15 m/s and of sub-cooling 5–50 K. High-speed video images are captured during quenching and are analyzed together with cooling curves with a view to having some information on the phase-change phenomena and heat transfer at the very beginning of the jet impingement.

2. Experiment

Fig. 1a shows the basic setup for the quench experiment, which is the same as used by Mozumder et al. [13,14]. The key components of the apparatus were a heated cylindrical test piece, a water jet, a number of electrical heaters and a spring-loaded shutter. The cylindrical test piece was steel or brass and had a diameter of 94 mm and a height of 59 mm. The test surface was polished and plated with a 5 μm layer of gold to reduce oxidation effects. After gold plating the surface roughness was measured to be about 7 μm for brass and about 18 μm for steel. The water jet issued from a 2 mm diameter nozzle located 45 mm away from the test surface. Three electrical heaters were used to heat the solid having a combined power of about 2.1 kW. Sixteen Chromel–alumel type thermocouples in two depths beneath the surface were embedded within the solid to record the thermal history as the block cooled. Eight of the thermocouples were located at a depth 1.9 mm from the surface and the other 8 were 5 mm from the surface. Radial positions of the thermocouples are 0, 5, 10, 16, 22, 28, 34 and 40 mm

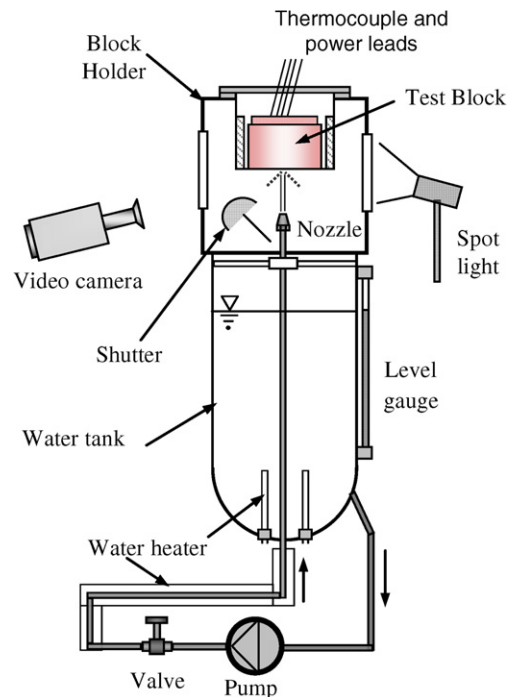


Fig. 1a. A schematic of the experimental setup.

from the center of the test surface with a maximum of 0.5 mm error. The thermocouples were connected to a multi-channel amplifier and then to a personal computer to store the readings during quenching. Readings were taken at a frequency of 10–20 Hz, which was as fast as could be justified given the response of the sensors and still slow compared with the 8 ms required by the AD card to scan all 16 channels. The entire experimental test section shown in Fig. 1b was enclosed in a nitrogen atmosphere as an additional measure to reduce oxidation. However, in order to take clear photographs it was necessary to open the door allowing some oxygen to enter the system.

The experimental procedure was to first fill the liquid tank with around 20 L of distilled water. The test surface then was wiped and cleaned with acetone. The block and the water were heated to the desired initial temperatures

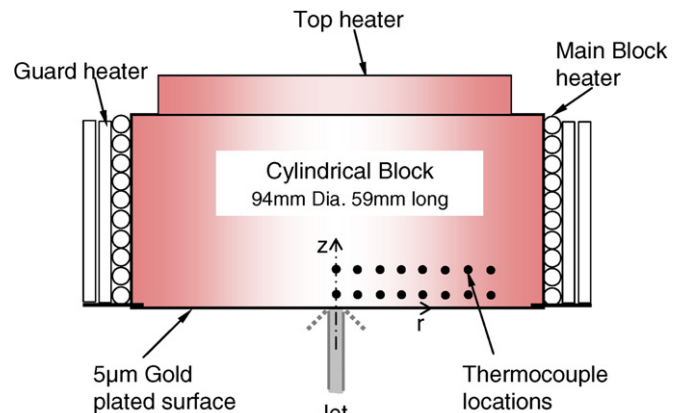


Fig. 1b. Detail of the test block.

while continuously pumping the water through a closed loop cycle with the shutter closed. When the thermocouples indicated that solid had reached the required temperature, the heaters were switched off. Due to rapid heating, there was a small temperature gradient in the solid, which caused the temperature near the surface to continue to rise from 3 to 4 °C above the intended initial condition after the power to the heaters was disconnected. During the next 3–4 min, the temperature gradients in the solid evened out and the solid began to cool slowly and uniformly at about 0.1 K/s. When it had cooled to the desired initial condition, the shutter shown in Fig. 1a was opened allowing the jet to strike the surface. At the same time a high-speed video camera of 10,000 frames per second was employed to capture the flow patterns.

3. Results and discussion

A high-speed video camera captured images of boiling and flow phenomena at the early stages of jet impingement quenching of the test block mentioned in the previous section. The embedded thermocouples also recorded temperature response during quenching. The temperature responses were then used by the inverse heat conduction method of Monde et al. [19] in order to predict surface temperature and heat flux. The video images are first analyzed in this section. The cooling curves at the center for different experimental conditions are presented subsequently with a view to understanding the quench phenomena and finding characteristic regions.

3.1. Video observation

A sequence of video clips at the early stages (from 3 ms to 3 s) during quenching of a steel block ($T_{b0} = 500\text{ °C}$) by a 5 m/s – 80 °C water jet is included in Fig. 2(a). Soon after jet impingement, a circular shiny (mirror like) liquid sheet was observed at the center of the block as shown up to 30 ms (for some other experimental conditions this phenomenon persisted for several seconds). During this period, the flow was very calm and quiet and no boiling sound was heard by an unaided ear. It seems that the jet hardly made contact with the surface at this stage. At the start there may be a brief solid–liquid contact at the center where bubbles form, coalesce and make the jet slide over the hot surface resulting in a flat sheet. When the size of the shiny sheet reaches its limit, numerous tiny liquid droplets form at its fringe as shown in the figure for 30 ms. A little later (around 200 ms), the above mentioned shiny liquid sheet started disappearing and the jet contacted the surface directly. Boiling might have occurred due to heterogeneous and/or homogeneous bubble nucleation and some liquid was found to be splashed away at an angle from the surface as shown in Fig. 2(a) at 200 ms and 500 ms. More rigorous contact was evident after 500 ms and a growing wet patch formed at the center. The liquid was deflected more as time progressed because of the possible interaction between the jet and the bubbles generated in the wetted area.

Fig. 2(b) exhibits a completely different sequence of video images during 3 ms to 4 s of quenching of a brass block initially heated to 550 °C by a 5 m/s – 50 °C jet. Within 30 ms, the flow was found explosive and noisy

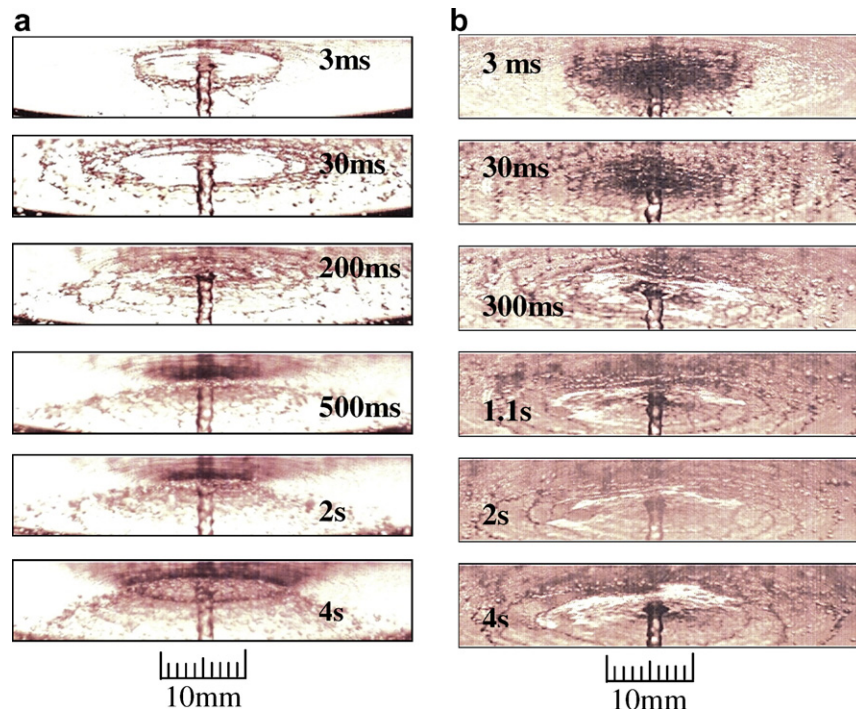


Fig. 2. Video clips during quenching of steel and brass blocks by 5 m/s jet: (a) 500 °C-steel quenched by 80 °C jet, (b) 550 °C-brass quenched by 50 °C jet.

where splashed liquid moved away in all possible directions. During 200–300 ms, oscillating sheet flow was observed. After about 500 ms a nearly stable sheet flow was evident. Unlike the flow for steel as shown in Fig. 2(a), no wet patch was found in the early stages of quenching. It took about 170 s to form a growing wet patch and to have a flow pattern the same as shown in Fig. 2(a) for 500 ms. It should be mentioned finally that the time duration until the wet patch starts growing strongly depends on the quenched material and thermal-hydraulic condition of the jet.

3.2. Flow patterns

Based on the video images during quenching steel and brass blocks, different flow patterns of the types from photos A to F have been identified as depicted in Fig. 3. The characteristics of the flow patterns are explained below.

Type A: Highly chaotic two-phase flow occurs as soon as the water jet is impinged on a hot brass surface. Tiny bubbles may be formed during brief instants of solid–liquid contact. Resultant of the forces exerted by tiny bubbles splashes the liquid in all possible directions. The steel sur-

face does not show this type of pattern clearly. The higher value of the thermal parameter, $\rho c \lambda$, of the block material and the higher surface temperature may in part be responsible for this type of flow pattern. Both heterogeneous and homogeneous bubble nucleations are considered possible at this stage.

Type B: Stable film boiling occurs on the steel surface as soon as the jet strikes it. This is quiet. At start there may be a brief solid–liquid contact at the center where bubbles form, coalesce and make the jet slide over it resulting in a flat liquid sheet. Or some pre-existing hot air at the surface and vapor formed at the top surface of the impinging jet play an important role in making the jet slide over to have a shape as shown. The study of free surface liquid sheets by Shoji [20] may be referred here for more information. As shown in Fig. 3 (type B), at a radius of about 10 mm, the sheet breaks into droplets that move outwards at angles of 5–10° from the surface. Brass blocks do not generally exhibit this, but some of the first quench experiments on brass blocks where gold plating was in good condition showed this pattern. The lower value of the thermal parameter, $\rho c \lambda$, of the block material, good surface condition and higher block temperature may in part be

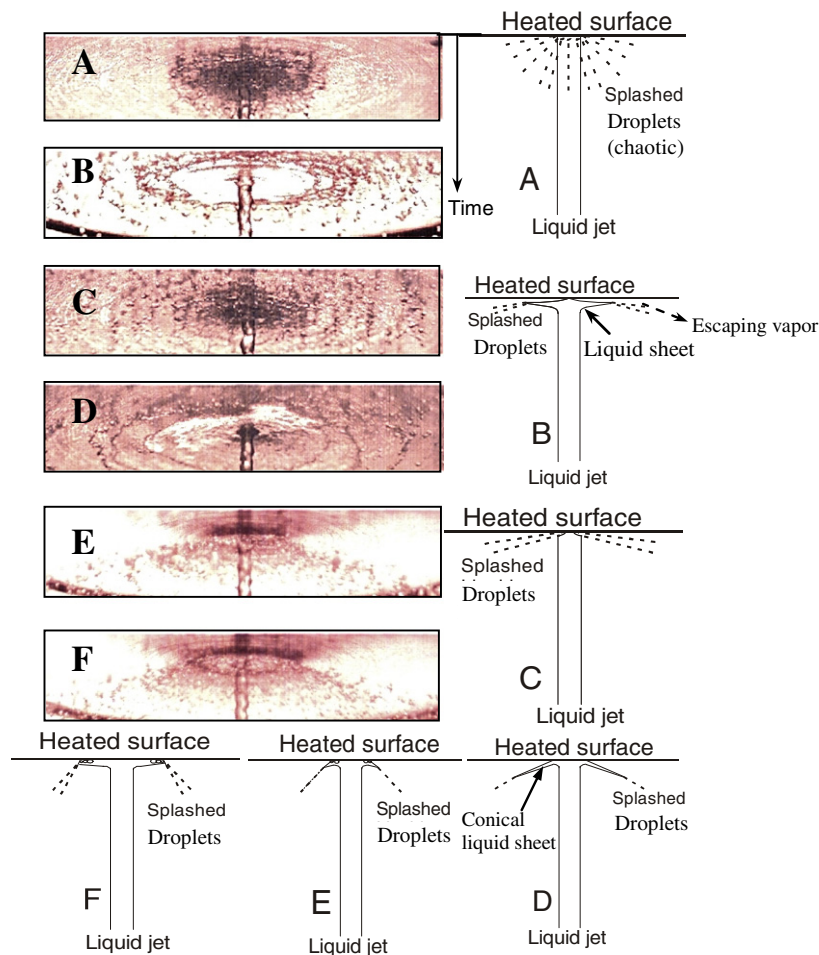


Fig. 3. Flow patterns identified from video observation.

responsible for this type of flow pattern. Both heterogeneous and homogeneous bubble nucleation may also be considered possible at this stage.

Type C: As time passes on, the surface temperature goes down because of the heat transfer and two-phase phenomena mentioned for type A or B. A little longer solid–liquid contact makes a small wet patch surrounding which a considerable number of isolated bubbles form that compels the jet to be directed outward with splashed liquid droplets as shown. For this type of flow pattern, the angle between surface and the line of splashed droplets varies from 10° to 15° . This flow pattern is common for both steel and brass surfaces. For steel this follows type B, while for brass it occurs after type A in most of the cases. Heat transfer by transition boiling (originated by both homogeneous and heterogeneous nucleation) may be possible for a brief period of time at this stage.

Type D: This is a conical sheet flow pattern observed after C-type. It is a delicate flow pattern occurring under favorable thermal-hydraulic conditions. Solid temperature, liquid flow rate, its subcooling and surface tension seem to play important roles on its formation. It seems that a small wet patch (larger than that for the type C) remains in contact with the surface for a considerable period of time at the center and helps produce more bubbles that deflect the jet further from the impinging surface and make an angle of about 15 – 20° . The hydrodynamic pressure of the impinging jet does not allow vapor to splash the thick liquid at the fringe of the wet patch. Rather the vapor forms a stream and escapes along the solid surface. The resultant of the forces exerted by the jet and the escaping vapor helps form this flow pattern having a conical liquid sheet. For the cases where jet velocity is low and jet subcooling is high, this flow is almost always common. Transition boiling (originated by both homogeneous and heterogeneous nucleation) may be the possible mode of heat transfer at this stage.

Oscillations between D and C type flow patterns were observed during quenching of high temperature surfaces considered in this study. Woodfield et al. [12] also found and explained these phenomena during jet quenching brass block initially heated to 300°C . They also presented the statistics of the sheet flow appearance. They mentioned that the maximum cycle took a little over one second and the average frequency of the cycle was 2.88 Hz.

Type E: As the surface temperature decreases with time, the wet patch grows more having a size larger than about double of the jet diameter and stagnates for a certain time, helps generate more and more bubbles near its fringe. At the fringe of the wet patch, the jet hydrodynamic pressure almost disappears and also the liquid film thickness becomes thin. These allow the vapor stream to break the conical liquid sheet (which is present in Type D) into splashed droplets that are more steeply deflected from the surface. On the formation of this flow pattern a sharp change in boiling sound was heard indicating that the wet patch is about to move along the radial direction. The angle between the surface and the splashed droplets

increases a little more (20 – 25°). Both fully developed nucleate boiling and transition boiling are established near the region where the splashed droplets are generated.

Type F: As the surface temperature of the wet patch and its outskirts goes down further, the wet patch starts growing along the radial direction. The angle between the surface and the splashed liquid again increases further having values ranging from 25° to 40° and it approaches to nearly 90° as the wet patch reaches the circumference. This type of flow pattern is characterized by the presence of different modes of heat transfer, viz. developing nucleate boiling in the wet patch, fully developed nucleate boiling at the fringe of the wet patch and transition boiling near the wetting front. Single phase convection is also possible for the cases where jet wets nearly the whole area of the impinging surface.

Neither steel nor brass exhibited all the abovementioned flow patterns during jet quenching. For steel B, C, E and F types of flow patterns were common, while for brass quenching A, C, D, E and F types of flow patterns were observed. It is worth mentioning that the surface finish and its aging play an important role in exhibiting the different types of flow pattern as explained above. Furthermore, the gold plating on the impinging surface was found partly washed away after every experimental run. Therefore, a poor repeatability of the duration and appearance of the flow patterns for a given initial temperature, jet velocity and subcooling was found in this experiment.

3.3. Boiling characteristics

During jet quenching, the modes of heat transfer can be well understood with the help of a boiling curve that shows the heat flux distribution with wall superheat. Fig. 4 shows a typical boiling curve at a radial position of 5 mm during quenching a 500°C steel block by an $80^\circ\text{C} - 5\text{ m/s} - 2\text{ mm}$ water jet. The heat flux increases with wall superheat, reaches the maximum of 2.76 MW/m^2 when wall superheat is about 127.3 K, and then decreases until wall superheat becomes 474 K after which a sharp increase in heat flux is evident. Interpreting this result from a classical view point, the nucleate boiling regime may be considered with wall superheats between 10 and 127.3 K, the transition boiling regime with wall superheat between 127.3 and 474 K and the film boiling regime with wall superheat beyond 474 K which is commonly considered as minimum film boiling point (MFB) or Leidenfrost point (LFP). The nucleate boiling prediction by Rohsenow [21] for pool boiling is shown in this figure to understand the similar boiling phenomena during jet quenching. To transfer the same amount of heat in the nucleate boiling regime having wall superheat more than 25 K, the surface temperature remains higher for jet impingement boiling compared to pool boiling. In other words, the heat transfer rate is lower for jet quenching at a certain wall superheat more than 25 K compared to pool boiling. This contradicts with the classical heat transfer character of steady-state pool boiling and forced convection boiling. This discrepancy may be

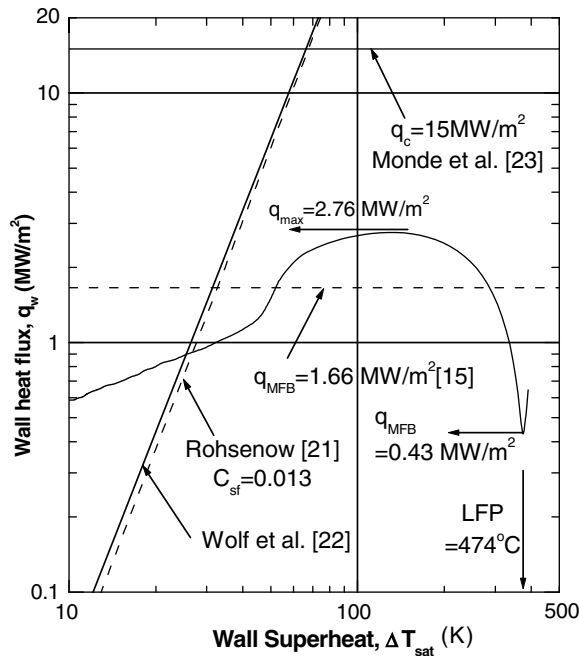


Fig. 4. A typical boiling curve at $r = 5$ mm (steel block of $T_{bo} = 500$ °C quenched by 80 °C – 5 m/s jet).

attributed to the complex hydrodynamics of jet and transient nature of heat transfer in the present study. Again, the nucleate boiling prediction by Wolf et al. [22], as also shown in Fig. 4, during plane jet impingement quenching shows good agreement with steady pool boiling, but deviates much from present jet quench character.

The value of q_{max} in jet quenching is much lower than the critical heat flux (q_c) for steady-state jet impingement boiling predicted by Monde et al. [23] as shown in Fig. 4. The reason why the value of q_{max} is lower than the Monde et al. prediction is mainly because of the heat transfer limitation caused by thermal properties of the block quenched as mentioned by Mozumder et al. [14]. The minimum film boiling heat flux (q_{MFB}) for the experimental conditions is about 0.43 MW/m² whereas it is about 1.66 MW/m² as predicted by Ishigai et al. [15]. It is worth mentioning that the prediction of Ishigai et al. [15] is a correlation developed for jet velocity less than 5 m/s.

It may be useful to note that the surface temperature during at the early stages of jet quenching remains high enough to exhibit film boiling for all the experimental conditions in the present study. But the boiling curves do not always show up the film boiling regime. This may be because of inaccuracy of the heat flux prediction resulting from the slow response of the thermocouples. It may also be useful to mention that brief random solid–liquid contacts are still possible at the early stages where stable film boiling is expected [16].

3.4. Cooling curves

Fig. 5 shows the variations of surface temperature, heat flux and cooling rate at a radial position of $r = 5$ mm dur-

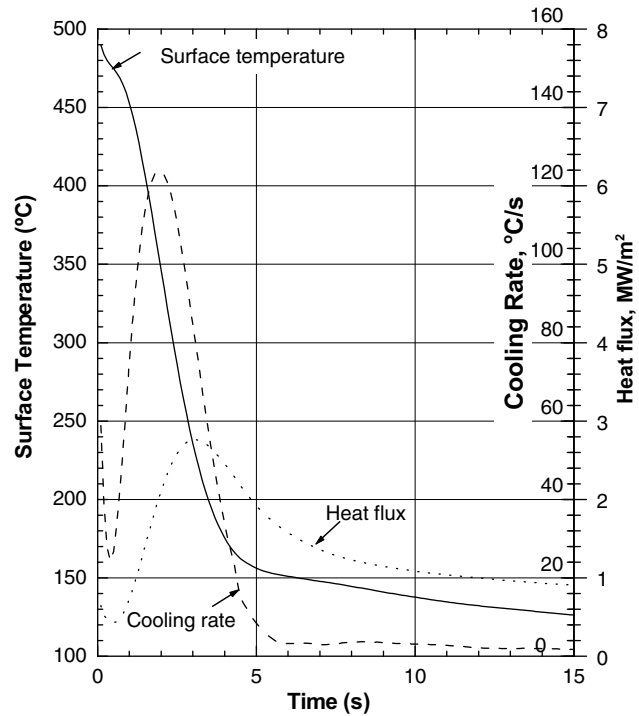


Fig. 5. Variation of temperature and heat flux at $r = 5$ mm during quenching of a 500 °C-steel block by 80 °C – 5 m/s jet.

ing quenching the 500 °C steel block by an 80 °C – 5 m/s jet. It is worth mentioning that the cooling rate considered here is based on the temperature measured by the thermocouples of response time close to 0.1 s. Therefore, average values over a period of this order for both temperature and cooling rate should be understood in the present context. If it could be possible to record surface temperature changes during a couple of microseconds at the beginning by an ultra-fast response temperature probe, which is perhaps not available yet, the cooling rate for jet impingement might be found to exceed the heating rate investigated hitherto in understanding spontaneous nucleation and vapor explosion. If one looks into liquid side when it suddenly contacts a hot solid, the heating rate takes an infinite value at the instant of contact.

It is found from Fig. 5 that the average cooling rate is as high as 60 °C/s at the very beginning of jet impingement due to initial transients [13], drops to 22 °C/s due to film boiling within 0.5 s and again enhanced to 124 °C/s after 1.9 s due to vigorous nucleate boiling. The possible heat transfer modes are film boiling, transition boiling and fully developed nucleate boiling as quenching proceeds from the beginning of jet impingement to 3.1 s (where q_{max} occurred). The surface heat flux reaches its maximum of $q_{max} = 2.76$ MW/m² while the cooling rate becomes maximum (124 °C/s) 1.9 s after the jet first impinged on the surface. For uniform cooling of a lumped solid the maximum heat flux and maximum cooling rate should occur simultaneously. However, the present circumstance involves steep temperature gradients in a two-dimensional solid. The 1.2 s

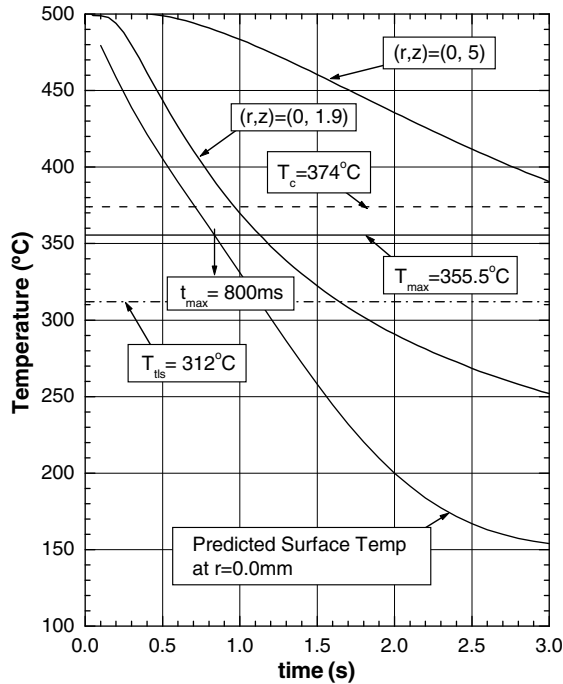


Fig. 6. Cooling curve during quenching of a 500 °C-steel block by 80 °C – 5 m/s jet.

time gap can be attributed to strong heat conduction to the cooler central region before occurrence of the maximum heat flux on the surface at the radial position shown in Fig. 5.

Fig. 6 exhibits changes of solid temperature with time at the center and at different depths of a 500 °C steel block during quenching by a 80 °C – 5 m/s water jet. The upper two solid curves are the temperature responses within the steel block at the depths of 1.9 mm and 5 mm beneath the impinging surface, while the lowest one is the surface temperature predicted by the inverse heat conduction solution [19]. The different horizontal lines represent some limiting temperatures. The dashed line is the critical temperature T_c of water, while the dash-dot-dash line shows the thermodynamic limit of liquid superheat T_{tls} suggested by Lienhard [24] for the quench condition given in Fig. 6. Carey [25] also suggested the value for T_{tls} to be 306 °C on the basis of kinetic homogeneous nucleation theory. The solid horizontal line is the limiting surface temperature T_{max} that allows stable solid–liquid contact during quenching. Considering the thermodynamic limiting temperature (spinodal limit) T_{tls} as the interface temperature, Eq. (1) can be used to calculate the maximum solid temperature T_{max} by presuming jet impingement on a solid surface as a two-semi-infinite-body contact problem [26]:

$$\frac{T_{max} - T_{tls}}{T_{tls} - T_1} = \sqrt{\frac{(\rho c \lambda)_l}{(\rho c \lambda)_s}} \quad (1)$$

where ‘ ρ ’, ‘ c ’ and ‘ λ ’ are, respectively, the density, specific heat and thermal conductivity and the subscripts ‘l’ and ‘s’ stand for liquid and solid, respectively.

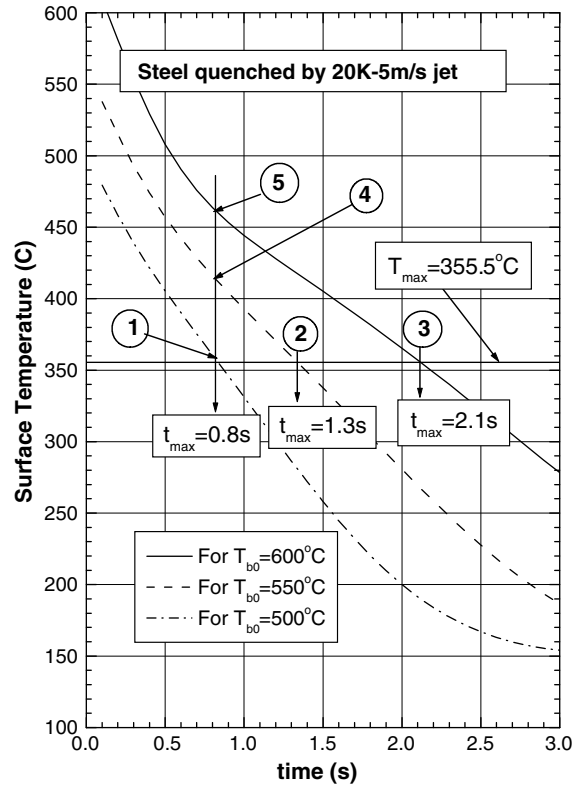


Fig. 7. Effect of T_{b0} during quenching steel blocks by 80 °C – 5 m/s jet.

It is learned from Fig. 6 that the surface temperatures were well above the $T_{max} = 355.5$ °C just after jet impingement having no sustainable solid–liquid contact and became equal to T_{max} at about $t_{max} = 800$ ms beyond which the surface cooled below this limiting temperature maintaining well solid–liquid contact during the quench. Neither video observations nor measured solid temperatures can tell us exactly what is happening within t_{max} after the quench. It is speculated that film boiling with intermittent wet and dry phenomena may be dominating heat transfer mode at this stage of quenching. A conceptual explanation of the early stages where the surface temperature is above the T_{max} will be presented in Section 3.6.

The time t_{max} when surface temperature becomes equal to T_{max} strongly depends on the experimental conditions. The higher the initial block temperature, the greater is the value of t_{max} as depicted in Fig. 7 which exhibits the changes of surface temperature at the center during quenching of a steel block (initially heated to 500–600 °C) by a 80 °C – 5 m/s water jet. The video images at (T_{max} , t_{max}) encircled as 1, 2 and 3 in the figure are all of C type given in Fig. 3. While flow patterns at t_{max} having a temperature higher than T_{max} (for the cases of encircled 4 and 5) are found oscillating between C and D. Again, the higher the jet velocity and subcooling, the lower is the value of t_{max} . The higher cooling potential for higher jet velocity and subcooling makes t_{max} smaller.

Fig. 8 compares the cooling phenomena at the center of brass and steel blocks for identical quench conditions of

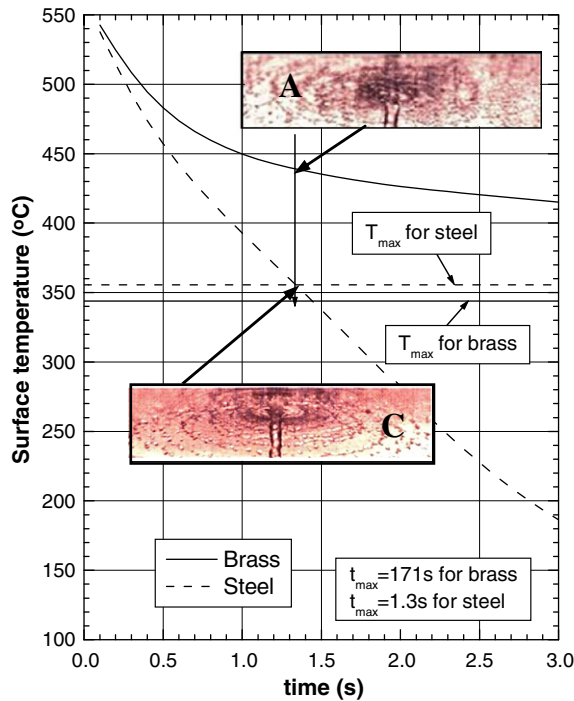


Fig. 8. Comparison of cooling curves of steel and brass blocks initially heated to 550 °C and quenched by 80 °C – 5 m/s water jet.

$T_{b0} = 550\text{ °C}$, $T_1 = 80\text{ °C}$, $u = 5\text{ m/s}$. Two horizontal lines in Fig. 8 show the T_{\max} for steel and brass. The surface of the steel block quickly cooled down to 200 °C by 3 s after jet impingement while the surface temperature for brass is well above 400 °C within this time as shown in Fig. 8. It is worth mentioning that the amount of heat transfer for brass was much more than that for steel for the same quench condition even though the surface temperature for brass is higher. This indicates that the steel block was cooled locally near the surface while a greater volume of the brass block was cooled during the same time period. In other words, the steel block was skin-cooled down to much lower temperature as mentioned above. The thermal properties (ρ , c , λ) of the block play an important role in this regard.

The surface temperature crosses the T_{\max} line after 1.3 s for the steel block as shown in Fig. 8 while for brass it does the same after 171 s (not shown). Two video images added here exhibit the flow patterns 1.3 s after jet impingement when the surface temperature of steel equals to T_{\max} . The images suggest that the jet made a sustainable contact with the steel surface and that it exploded violently in contact with the brass surface whose temperature is well above the limiting temperature T_{\max} .

Fig. 9 is a cooling curve giving some more information of the quench phenomena of a 550 °C-brass block when a 50 °C – 5 m/s water jet was impinged on it. This shows that the surface was cooled down to T_{\max} in 1.2 s, from T_{\max} to T_w^* in 98.8 s and from T_w^* to 150 °C in next 15 s. The T_w^* is the surface temperature when a stagnant wet patch at the center starts growing and t^* is the time at

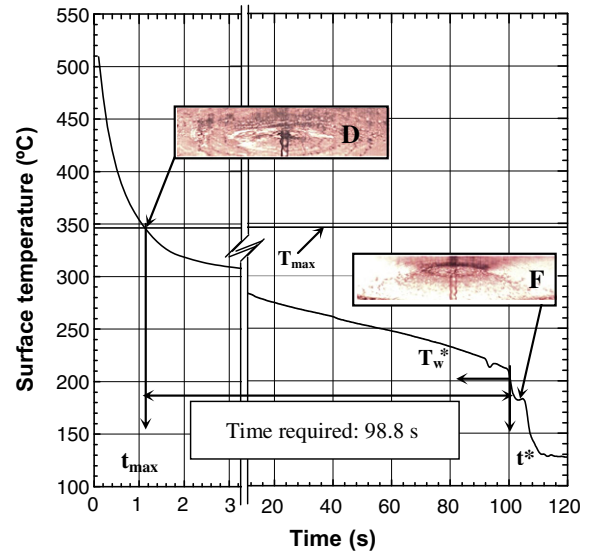


Fig. 9. Characteristics of 550 °C-brass block quenched by 50 °C – 5 m/s jet.

T_w^* . Therefore, the cooling may be characterized by the faster rate in the early region, the slowest in the middle region and again faster in a brief region followed by a slower rate when the surface temperature is below 130 °C as depicted in Fig. 9. The respective heat transfer modes are unstable film boiling with oscillating wet and dry phenomena, stable film boiling, transition boiling extending to vigorous nucleate boiling and single phase convection. Two video images shown in Fig. 9 display the flow situation at the transitions: one at (t_{\max} , T_{\max}) having conical sheet flow of liquid (Type D) and the other beyond the transition at (t^* , T_w^*) having a growing wet patch with vigorous nucleate boiling at the fringe (Type E).

3.5. Characteristic regions

On the basis of cooling rate and its transitions at T_{\max} and T_w^* , three different characteristic regions are tentatively identified as shown in Fig. 10. The characteristics of these three regions are explained below:

Region I: This is the cooling region that happens in the very early stages of quench between 0 (start) and t_{\max} during which the surface temperature remains more than or equal to T_{\max} . Unstable film boiling/explosive boiling may be the heat transfer mode; some brief solid–liquid contacts make the surface cool down to the interface temperature T^* and explosive vaporization of liquid makes the surface dry again. The flow pattern changes from type A to type C with time for brass in this region, while for steel the changes in flow pattern from type B to type C are observed as quenching progressed. The flow pattern of the type D is observed for a few cases of steel and brass where surface temperature seems to be pretty close to T_{\max} .

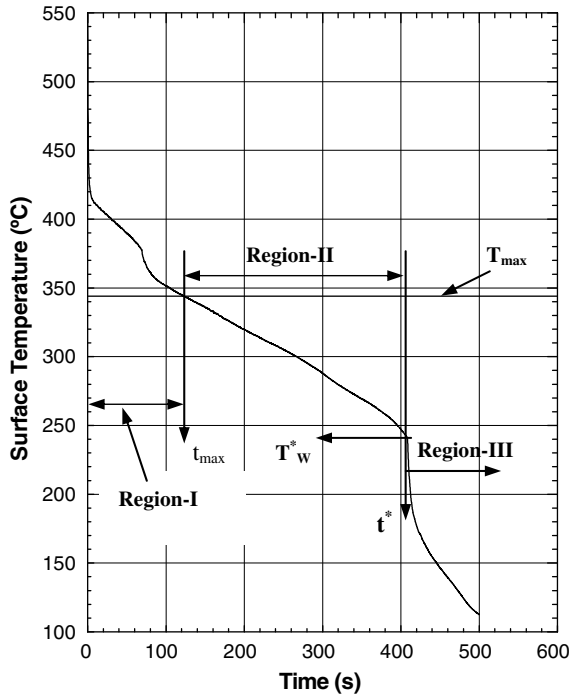


Fig. 10. Characteristics cooling regions during jet impingement quenching.

Region II: This is the quench period between t_{max} and t^* during which the surface temperature remains within the range from T_{max} to T_w^* maintaining a stable contact with the impinging jet in a certain region at the center. At the surrounding of this well wetted central region, there forms an annular region that becomes repetitively wet and dry and experiences transition boiling. Therefore, the extent of wetting oscillates at a certain frequency and the jet stands still making a stagnant wet patch until the surface cools down to T_w^* at which the central wet patch starts growing quickly. As shown in Fig. 10, the surface is cooled slowly in this region due to limited wetted area. The flow patterns are found oscillating between types C and D in this region with a decreasing frequency of oscillation. This region ends up with exhibiting E type of flow pattern when the surface is cooled down to T_w^* .

Region III: It starts after t^* when the surface is cooled quickly such that the surface temperature drops much from the T_w^* . This region starts with transition boiling and ends up with nucleate boiling. The stagnation wet patch at the center starts growing at the very beginning of this region. More stable solid–liquid contact and favorable heat transfer rates from the surface make the wetting move forward in this region. The maximum heat flux occurs during this period [14]. The flow pattern in this region is type E at the start and type F at the end.

3.6. Cooling phenomena at the early stages

Neither video observation nor temperature history during jet impingement quenching of a high temperature

surface help find a clue in understanding the phenomena that happen at the early stages. Even though the surface temperature during the early stages is well above the thermodynamic limiting temperature (T_{max}) that allows solid–liquid contact [8], the jet impacts the surface by the hydrodynamic forces and bounces immediately because of possible vapor formation during the brief contact making the surface dry again. Some amount of heat is transferred during these events of wet and dry which may continue at different frequencies until the surface temperature becomes equal to a certain temperature such as T_{max} and a sustainable solid–liquid contact may be established.

Fig. 11 demonstrates a concept of how the surface temperature may change with the above mentioned wet and dry phenomena within first few of microseconds of jet impingement quenching. The dark solid line in Fig. 11 is the possible change in solid surface temperature during first two cycles of wet and dry events in the early stages of quenching. Other solid horizontal lines drawn in the figure are T_{b0} , T_{max} , T_{lts} and T_l . The upper dashed line is the average temperature that may be predicted by the inverse heat conduction solution [19] using the thermocouple readings. The dotted line is the possible variation of liquid surface temperature during brief wet and dry events at the early stages. The first cycle of wet and dry (a–b–c–d) may be explained as follows:

- (1) a–b: The surface instantaneously assumes the interface temperature T^* as the liquid comes in contact with it. Both solid surface and liquid are considered as one-dimensional semi-infinite bodies at this stage and the Fourier heat conduction solution by Carslaw

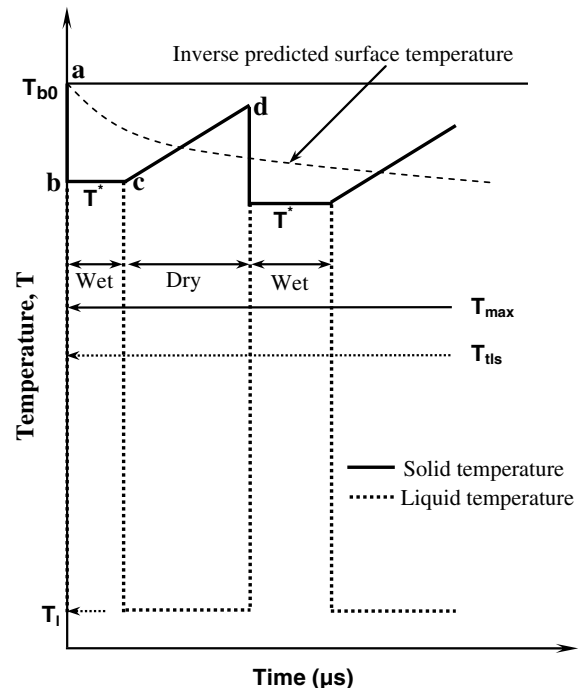


Fig. 11. Possible temperature oscillation in Region I.

and Jaeger [26] can be used to calculate the value of T^* using Eq. (2):

$$\frac{T_{b0} - T^*}{T^* - T_1} = \sqrt{\frac{(\rho c \lambda)_l}{(\rho c \lambda)_s}} \quad (2)$$

- (2) b–c: Solid–liquid contact may be maintained for less than a microsecond and heat is transferred to the liquid by conduction. The surface temperature at this brief contact may be assumed constant as shown. It is interesting to note that liquid is considered to be in liquid state at T^* which well above thermodynamic limit of liquid superheat, T_{ils} . It is thought that liquid molecules come in contact with the surface at this stage and the conducted heat is stored in the molecules at a depth of a few nanometers. The stored heat makes enough molecules excited to give rise homogeneous bubble nucleation/explosive boiling whose mechanism is not clearly understood yet.
- (3) c–d: Liquid molecules are momentarily transformed into vapor molecules due to possible homogeneous nucleation/vapor explosion and make the solid surface dry as the vapor molecules prevent the jet from making any contact with the solid surface until those escape or condense to liquid again. The temperature of the solid surface is recovered as shown because of heat conduction from the region far from the surface. The liquid is also cooled and the generated vapor is condensed quickly because of fresh supply from the jet. The jet comes in contact with the surface again to repeat the cycle of wet and dry.

During the events mentioned above, the surface gets wet and dry alternately with a certain frequency not ascertained yet. These events repeat with increasing period of solid–liquid contact as the surface cools. In other words, the average surface temperature decreases as the time passes on and the above events take relatively longer time to repeat. Therefore, the period of the cycle becomes longer. An accurate prediction of the change of surface temperature and its frequency may help predict surface heat flux correctly. This could eventually tell us about the type of boiling occurring at the early stages.

While the pattern shown in Fig. 11 is speculative, there is some evidence that a similar kind of phenomenon has been observed by others during transition boiling. Cokmez-Tuzla et al. [18] conducted an analysis for the quantitative characteristics of liquid–wall contacts in the vicinity of quench fronts for flow boiling, with emphasis on the time fraction of contacts. In order to detect and record potential liquid contacts in the vicinity of an advancing quench front, a special rapid-response contact probe was utilized whose response time was determined to be better than 0.1 ms to sense 99% of any sudden temperature change. The sampling frequency of the probe was 16,000 data points per second. They observed that the surface temperature initially stayed at high superheats decreased gradually with intermittent

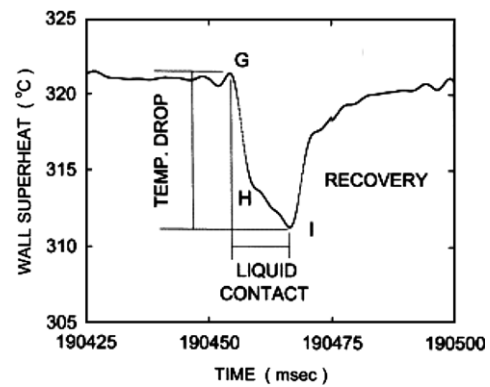


Fig. 12. Contact probe signal collected by Cokmez-Tuzla et al. [18].

sudden drops and recoveries. Fig. 12 exhibits a magnified view of a single event of contact maintained for about 15 ms. The faster cooling of the surface between points G and I as shown in Fig. 12 is because of the liquid in contact with the wall and can be approximated by a suitable function of $t^{1/2}$ to have an estimate of the surface heat flux on this basis of heat conduction analysis. For a brief contact of liquid for 15 ms, the surface heat flux can be calculated as 3.5 MW/m^2 by considering the contact probe to be a semi-infinite solid. This value of heat flux is much less than that can be calculated considering the phenomena at the Region I during jet impingement as explained above for Fig. 10. This type of observation and surface temperature change of Cokmez-Tuzla et al. [18] are common in the transition boiling region where liquid contacts solid surface for a couple of milliseconds and above as in the cases of Region II and Region III mentioned in Fig. 10. In the present early stage consideration (Region I of Fig. 10), the solid–liquid contact may be maintained for less than a microsecond as shown in Fig. 11 from b to c and so forth.

One obvious weakness with the model in Fig. 11 from b to c is that the assumption of the sudden contact of two semi-infinite bodies leads to an infinite heat flux, which is not possible due to the fact that liquid is made up of molecules requiring a finite amount of heat for phase-change. Therefore, we expect that in the future studies the ultimate limit to maximum heat flux based on molecular dynamics will also play an important role. In such a case, the interface temperature T^* calculated by Eq. (2) may be taken as temperature boundary and the maximum value of the maximum heat flux predicted by Gambill and Lienhard [27] may be taken as heat flux boundary. Solving the model for a couple of microseconds can give the temperature distribution in several nanometer depth of the liquid in contact and a clue in better understanding the boiling mechanism at the early stages may be obtained. Further investigation regarding this mechanism is indispensable.

4. Conclusions

Jet impingement quenching phenomena of hot surfaces near $600 \text{ }^\circ\text{C}$ by video observation and surface temperature

history have been presented in this paper. The outcomes of this study can be enumerated below:

1. The jet impingement quenching came up with different types of flow patterns depending on the surface temperature and material. Each of flow patterns has distinct hydrodynamic and boiling character.
2. The thermodynamic limit of liquid superheat T_{tfs} tells about the maximum temperature T_{max} that permits stable solid–liquid contact during quenching. The temperature T_w^* at the resident time t^* delineates the commencement of wetting movement and the onset of rapid cooling.
3. Three different characteristic cooling regions are identified during jet impingement quenching on the basis of cooling rate and its transition at T_{max} and T_w^* . The temperature measurements and video observation and their subsequent analysis are not enough in understanding the flow and boiling phenomena during the early cooling region of jet impingement.
4. At the early cooling region where the surface temperature is above T_{max} , the jet impacts the surface by the hydrodynamic forces and bounces immediately because of possible vapor formation by homogeneous nucleation/explosive boiling during the brief contact and the impinging surface gets dry again. The possible cooling phenomena at early stages of jet impingement quenching are illustrated and explained considering appropriate changes in surface temperature during wet and dry events.

Acknowledgements

Authors gratefully acknowledge the support provided by the Japan Society for the Promotion of Science (JSPS) and for the ‘Grant-in-Aid for Scientific Research’, 2004.

References

- [1] D.H. Wolf, F.P. Incropera, R. Viskanta, Jet impingement boiling, *Adv. Heat Transfer* 23 (1993) 1–132.
- [2] M. Monde et al., Augmentation techniques and external flow boiling, in: S.G. Kandlikar, M. Shoji, V.K. Dhir (Eds.), *Handbook of Phase Change: Boiling and Condensation*, Taylor & Francis, 1999, pp. 331–342.
- [3] V.P. Skripov, *Metastable Liquids*, John Wiley & Sons, New York, 1974 (Chapter 3, 6).
- [4] A. Asai, Bubble dynamics in boiling under high heat flux pulse heating, *J. Heat Transfer* 113 (1991) 973–979.
- [5] J.R. Andrews, M.P. O’Horo, High speed stroboscopic system for visualization of thermal inkjet processes, in: J. Bares (Ed.), *Proceedings, Society of Photo-Optical Instrumentation Engineers (SPIE)*, vol. 2413, 1995, pp. 176–181.
- [6] V.P. Carey, A.P. Wemhoff, Thermodynamic analysis of near-wall effects on phase stability and homogeneous nucleation during rapid surface heating, *Int. J. Heat Mass Transfer* 48 (2005) 5431–5445.
- [7] V. Gerweck, G. Yadigaroglu, A local equation of state for fluid in the presence of a wall and its application to rewetting, *Int. J. Heat Mass Transfer* 35 (1992) 1823–1832.
- [8] H. Ohtake, Y. Koizumi, Study on propagative collapse a vapor film in film boiling (mechanism of vapor film collapse at wall temperature well above the thermodynamic limit of liquid superheat), *Int. J. Heat Mass Transfer* 47 (2004) 1965–1977.
- [9] B.D.G. Piggott, E.P. White, R.B. Duffey, Wetting delay due to film and transition boiling on hot surfaces, *Nucl. Eng. Des.* 36 (1976) 169–181.
- [10] J. Hammad, Y. Mitsutake, M. Monde, Movement of maximum heat flux and wetting front during quenching of hot cylindrical block, *Int. J. Therm. Sci.* 43 (2004) 743–752.
- [11] J. Hammad, M. Monde, Y. Mitsutake, Characteristics of heat transfer and wetting front during quenching by jet impingement, *Therm. Sci. Eng.* 12 (2004) 19–26.
- [12] P.L. Woodfield, M. Monde, A.K. Mozumder, Observations of high temperature impinging-jet phenomena, *Int. J. Heat Mass Transfer* 48 (2005) 2032–2041.
- [13] A.K. Mozumder, M. Monde, P.L. Woodfield, Delay of wetting propagation during jet impingement quenching for a high temperature surface, *Int. J. Heat Mass Transfer* 48 (2005) 5395–5407.
- [14] A.K. Mozumder, M. Monde, P.L. Woodfield, M.A. Islam, Maximum heat flux in relation to quenching of a high temperature surface with liquid jet impingement, *Int. J. Heat Mass Transfer* 49 (2006) 2877–2888.
- [15] S. Ishigai, S. Nakanishi, T. Ochi, Boiling heat transfer for a plane water jet impinging on a hot surface, *Heat Transfer* (1978) 445–450.
- [16] K.H. Chang, L.C. Witte, Liquid–solid contact during flow film boiling of subcooled Freon-11, *J. Heat Transfer* 112 (1990) 465–471.
- [17] N. Hatta, J. Kokado, K. Hanasaki, Numerical analysis of cooling characteristics for water bar, *Trans. Iron Steel Inst. Jpn.* 23 (1983) 555–564.
- [18] A.F. Cokmez-Tuzla, K. Tuzla, J.C. Chen, Characteristics of liquid–solid contact in post-CHF flow boiling, *Int. J. Heat Mass Transfer* 43 (2000) 1925–1934.
- [19] M. Monde, H. Arima, W. Liu, Y. Mitsutake, J.A. Hammad, An analytical solution for two-dimensional inverse heat conduction problems using Laplace transform, *Int. J. Heat Mass Transfer* 46 (2003) 2135–2148.
- [20] M. Shoji, Study of free surface sheet flow: Rep. 1, *Trans. JSME* 39 (321) (1973) 1568–1577 (in Japanese).
- [21] W.M. Rohsenow, A method of correlating heat-transfer data for surface boiling of liquids, *J. Heat Transfer* 74 (1952) 969–975.
- [22] D.H. Wolf, F.P. Incropera, R. Viskanta, Local jet impingement boiling heat transfer, *Int. J. Heat Mass Transfer* 39 (1996) 1395–1406.
- [23] M. Monde, K. Kitajima, T. Inoue, Y. Mitsutake, Critical heat flux in a forced convection subcooled boiling with an impinging jet, *Heat Transfer* 7 (1994) 515–520.
- [24] J.H. Lienhard, Correlation for the limiting liquid superheat, *Chem. Eng. Sci.* 31 (1976) 847–849.
- [25] V.P. Carey, *Liquid–Vapor Phase-Change Phenomena*, Taylor and Francis, New York, 1992 (Chapter 5).
- [26] H.S. Carslaw, J.C. Jaeger, *Conduction of Heat in Solids*, second ed., Oxford University Press, 2001, pp. 87–89.
- [27] W.R. Gambill, J.H. Lienhard, An upper bound for the critical boiling heat flux, *J. Heat Transfer* 111 (3) (1989) 815–818.